

Hardware-assisted Trusted Memory Disaggregation for Secure Far Memory

Taekyung Heo

Seunghyo Kang

Sanghyeon Lee

Soojin Hwang

Jaehyuk Huh

School of Computing, KAIST

Abstract

Memory disaggregation provides efficient memory utilization across network-connected systems. It allows a node to use part of memory in remote nodes in the same cluster. Recent studies have improved RDMA-based memory disaggregation systems, supporting lower latency and higher bandwidth than the prior generation of disaggregated memory. However, the current disaggregated memory systems manage remote memory only at coarse granularity due to the limitation of the access validation mechanism of RDMA. In such systems, to support fine-grained remote page allocation, the trustworthiness of all participating systems needs to be assumed, and thus a security breach in a node can propagate to the entire cluster. From the security perspective, the memory-providing node must protect its memory from memory-requesting nodes. On the other hand, the memory-requesting node requires the confidentiality and integrity protection of its memory contents even if they are stored in remote nodes. To address the weak isolation support in the current system, this study proposes a novel hardware-assisted memory disaggregation system. Based on the security features of FPGA, the logic in each per-node FPGA board provides a secure memory disaggregation engine. With its own networks, a set of FPGA-based engines form a trusted memory disaggregation system, which is isolated from the privileged software of each participating node. The secure memory disaggregation system allows fine-grained memory management in memory-providing nodes, while the access validation is guaranteed with the hardware-hardened mechanism. In addition, the proposed system hides the memory access patterns observable from remote nodes, supporting obliviousness. Our evaluation with FPGA implementation shows that such fine-grained secure disaggregated memory is feasible with comparable performance to the latest software-based techniques.

1. Introduction

Memory disaggregation has emerged to enable efficient utilization of memory capacity across system boundaries. The imbalance in memory utilization among virtual machines or user applications in a cluster necessitates memory capacity sharing among the nodes in the same cluster. Recent studies showed that RDMA-supporting networks can allow effective expansion of memory beyond a single node with the low latency and high bandwidth data transfers [18, 2, 46]. Furthermore, there have been several commercial proposals for new interconnects that support fine-grained direct memory accesses to remote memory nodes [10, 36, 6]. Such memory disaggregation re-

duces the total cost of ownership of data centers by avoiding over-provisioning of memory capacity for each node.

Although there have been recent studies to improve the performance of the disaggregated memory systems [2, 46, 4], its security aspect has not been thoroughly investigated. Unlike typical system designs based on localized memory, the disaggregated memory system opens the memory boundary beyond the conventional system limit, and thus the memory contents of a user application can exist across multiple nodes. In addition, a node must allow other nodes to access part of its memory, being forced to trust the behavior of other nodes. The current disaggregated memory systems allow only coarse-grained access controls of RDMA, which limit the flexibility of memory management. To allow fine-grained memory allocation, a large memory pool must be accessible among nodes, and thus the collective trustworthiness of all participating nodes must be assumed. In such cases, a security breach in a single node can potentially propagate to the rest of the nodes since their memories are shared.

To protect against such *vulnerability propagation*, the disaggregated memory poses several new challenges. First, the confidentiality and integrity of memory pages stored in remote nodes must be protected under vulnerable privileged software in the remote nodes. Second, when a node (*donor node*) donates part of memory for other nodes, its memory must be protected from any malicious attempt to access illegitimate regions of memory. Third, memory management must be fine-grained and flexible. Assigning one big contiguous chunk of memory for sharing leads to the inefficient utilization of memory capacity, which offsets the benefit of memory sharing for improving memory utilization. Finally, memory access patterns of memory user nodes must be indistinguishable from the donor node.

However, the current disaggregated memory studies do not fully address the aforementioned challenges. A common approach for disaggregated memory is to rely on RDMA supports in network interface cards for low latency accesses across networks. In such systems, the remote memory address is stored in the memory user node (*donee node*) for low latency RDMA accesses. On the donor side, RDMA memory regions can be allocated in one or a few big chunks of memory pool to rely on coarse-grained access validation of RDMA network devices. Secure fine-grained management of huge memory capacity is hard to be supported with the limited region-based access control.

To harden the disaggregated memory system, this paper proposes a novel hardware-assisted disaggregated memory

system. For each node, the trusted logic on the FPGA board provides the fine-grained access validation between different nodes. Based on the security supports of FPGA, our per-node memory disaggregation hardware engines form a trusted memory disaggregation system for secure page transfers. As the confidentiality and integrity of the FPGA logic and its states are guaranteed, the operations on the FPGA board are completely protected from vulnerable operating systems. In addition, the FPGA boards are connected with their own networks, which do not pass through the network stack of the vulnerable operating systems. The new hardware-assisted memory disaggregation system provides strong isolation among the participating nodes, and thus even if one of the nodes is attacked, it does not adversely affect the other nodes. Figure 1 presents the trusted FPGA-based disaggregated memory system.

To overcome the limitation of the current coarse-grained permission validation, the hardware engine provides a fine-grained page-granular access control. To allow low latency access, the OS of the donee node maintains the target page address in the remote node. However, the secure FPGA logic in the donor node checks the source of page requests and validates the access at page granularity. Such decoupling of address translation and permission validation allows fine-grained access validation without degrading the performance.

Another important aspect of security is the patterns of page accesses. Prior work showed that such coarse-grained fault address patterns can leak critical information [55]. As memory disaggregation systems such as CXL have fixed mappings between the donee’s address space and the donor’s address space, a donor can track the memory access patterns of donees. To hide the memory access patterns, our proposal relies on the swap subsystem of the Linux kernel, which allocates a new swap slot on every page swap. As a result, the mappings between two address spaces constantly change, breaking up the connection between two address spaces. In addition, with the assistance of FPGAs, TDMEM further obfuscates write memory access patterns.

We propose Trusted Disaggregated Memory, TDMEM, the hardware design for secure and fine-grained disaggregated memory. This new hardware-assisted system is implemented in a Linux system equipped with the Xilinx Alveo U50. The Linux kernel has been modified for the tight integration of TDMEM with the existing virtual memory system. Our evaluation shows that even with the security supports with fine-grained memory management, the performance degradation is minimized to 4.4%, compared to the prior best-performing RDMA-based disaggregated memory system.

The source codes for FPGA logic and Linux patch will become publicly available after publication. The main contributions of this paper are as follows:

- This paper discusses the potential security problem of disaggregated memory and proposes a hardware-assisted approach by using the secure FPGA technique.
- It overcomes the limitation of the current RDMA-based

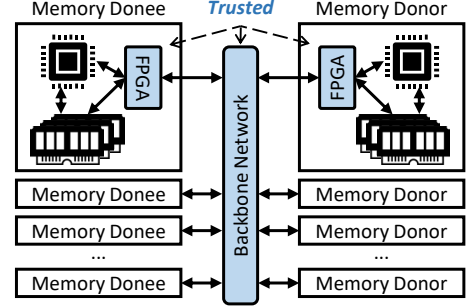


Figure 1: FPGA-based trusted disaggregated memory

approach with coarse-grained access control and provides the secure fine-grained page-level allocation.

- The hardware-assisted mechanism allows fast page transfers comparable to the prior mechanism based on region allocation.
- It obfuscates the memory access pattern of donees by exploiting the existing swap subsystem, so the data leaks by page access patterns are avoided.

The rest of the paper is organized as follows. Section 2 presents the background and motivation for hardware-assisted secure memory disaggregation. Section 3 discusses the threat model and security challenges. Section 4 presents the design of TDMEM, and Section 5 describes its implementation. Section 6 presents the experimental results with the real FPGA implementation. Section 7 discusses the related work, and Section 8 concludes the paper.

2. Background and Motivation

2.1. Memory Disaggregation

Memory disaggregation allows data to reside in remote memory. In general, a disaggregated memory system has several nodes connected with a high-speed network [18, 2, 46]. In this paper, we denote a node that donates its memory as a *donor* and a node that utilizes the memory of other nodes as a *donee*. A node can be a donor and a donee at the same time. From the perspective of a memory-consuming application, there are two types of memories: local memory and remote memory. The local memory is the memory in a donee that can be accessed without additional network latency and address translations. The remote memory is the memory donated by a donor.

Remote Direct Memory Access (RDMA), which enables direct memory access to the memory in a remote node, has been widely used in prior memory disaggregation studies [18, 2, 46]. The communication channel of RDMA is called a queue pair. A queue pair is composed of a send queue and receive queue. The communication between hosts can be done with the abstraction called *verbs*. Verbs are classified into two types depending on the involvement of a remote CPU: one-sided verbs and two-sided verbs. One-sided verbs do not require a remote CPU’s involvement, while two-sided verbs require. Therefore, one-sided verbs are more scalable than the other. However,

Name	Memory Protection	Secure Memory Alloc.	Fine-grained Memory Alloc.	Address Translation	Secure Translation	Memory Access Obfuscation
Intel CXL [10]	✓	✓	✗	Direct	✓	✗
Kona [4]	✗	✗	✗	Indirect	✗	✗
DeACT [26]	✗	✗	✗	Indirect	✗	✗
ThymesisFlow [40]	✗	✗	✗	Direct	✗	✗
AIFM [46]	✗	✗	✓	Indirect	✗	✗
Fastswap [2]	✗	✗	✗	Indirect	✗	✓
InfiniSwap [18]	✗	✗	✗	Indirect	✗	✓
TDMEM	✓	✓	✓	Indirect	✓	✓

Table 1: Comparison with prior studies

one-sided verbs are not a free lunch. A memory region must be registered to access memory with one-sided verbs. The memory registration takes tens of microseconds [16]. Accesses from remote nodes to a memory region are protected with a key, which is called `rkey`.

2.2. Requirements for Secure Memory Disaggregation

The distributed and shared nature of a disaggregated memory system imposes several requirements. In this subsection, we discuss four specific requirements that have been less explored in this field: memory protection, secure and fine-grained memory allocation, fast and secure address translation, and memory access pattern obfuscation.

Memory protection: The confidentiality and integrity of pages stored in remote memory must be guaranteed. As a donor has full control over donated memory, a donor may read or write any stored pages. Moreover, if a disaggregated memory system fails to isolate nodes due to design flaws or bugs, a malicious donee may read or write unauthorized pages. Therefore, pages should be encrypted before being swapped out to remote memory. In addition, any modifications to pages have to be detected to prevent reading contaminated pages. Reading contaminated pages may result in a malfunction of applications or privilege escalation.

Secure and fine-grained memory allocation: First, memory allocation metadata must be securely protected from adversaries. The metadata include the start address, size, and ownership of allocated memory. As these metadata are used for memory access control, tampering of memory allocation metadata may result in unauthorized reads or writes of memory. Second, memory allocation must be done at fine-granularity for efficient memory utilization. Coarse-granular memory allocation may fail to meet the fluctuating memory demands of applications, which results in wasted memory from internal fragmentation. Fine-granular memory allocation reduces the wasted memory from internal fragmentation.

Fast and secure address translation: Memory disaggregation involves mappings between a local address space and a remote address space. The local address space is used by a donee’s CPUs to access data in local memory, and part of the local address space can be backed by the remote memory in donors. As the address translations from a local address to a

remote address are in the critical path of accessing data, fast address translation is essential to achieve high performance. In addition to fast identification of remote addresses, secure address translation is critical to prevent a compromised donor from providing corrupted pages and to prohibit a malicious donee from reading unauthorized pages.

Memory access pattern obfuscation: The memory access patterns of donees must be hidden from a donor node. Even if a donor node can observe the memory access patterns, the patterns should not convey any critical information by obfuscating the memory access pattern. Many prior studies have shown that the disclosure of memory access patterns may leak critical information such as the access frequency of data and correlation between them [59, 22, 30]. Moreover, several practical software attack schemes based on memory access pattern detection were proposed [37, 22]. A malicious observer can extract information about the location of private data from memory access patterns, which can result in the revelation of private data.

2.3. Prior Studies in Memory Disaggregation

This subsection revisits and compares prior memory disaggregation studies to find whether the aforementioned requirements are met. Table 1 summarizes the prior studies with respect to the aforementioned requirements.

Memory protection: CXL offers the confidentiality, integrity, and replay protection of data. However, other prior studies support none of them. RDMA-based disaggregated memory systems [46, 2, 18] rely on the default memory protection mechanism, which is to authorize accesses to a memory region with `rkey`. However, as prior studies have shown [51, 45], `rkeys` are predictable because of the small key size and unrobust implementations. These security holes let a malicious donee read or write an unauthorized memory region.

Secure and fine-grained memory allocation: In CXL, memory allocation is done at the granularity of logical devices. CXL defines a memory pool device as a memory device that can be shared by multiple donees. A memory pool device can have 16 logical devices at maximum. The allocation of logical devices is advertised through a designated memory area, which is called `DVSEC`. As `DVSEC` can be configured by a fabric manager (FM) only, as long as the FM is securely

protected, memory allocation metadata are securely protected. Except for CXL, prior studies do not describe the security model for secure memory allocation. In short, the memory allocation of CXL is secure but done at coarse-granularity.

The security feature for memory allocation is not clarified in the other studies. Moreover, most prior studies allocate memory at coarse-granularity in the initialization stage. ThymesFlow allocates memory at the unit of a section, which is the memory management unit in the sparse memory model of the Linux kernel. The default section size is set to 1TB according to its specification. Kona allocates memory using a coarse-granular slab. Fastswap reserves memory in a donor where the memory size matches the size of the swap device size of the donee. The reserved memory in the donor cannot be shared with other donees. Unlike the other studies, AIFM allocates memory at object-granularity on demand. However, it loses transparency, mandating modifications to the user applications.

Fast and secure address translation: Prior studies can be classified into two types according to the existence of additional address space between a local address space and a remote address space. The studies without additional address space are classified as *direct*, and others are classified as *indirect*. Direct has an advantage in terms of performance because it can avoid additional address translations. However, it may weaken the security model by exposing the physical address space of a donor to donees directly. Moreover, donees may suffer from the leak of memory access patterns as the mappings between the local addresses and remote addresses are fixed. CXL and ThymesFlow adopt direct translations. Kona is classified as indirect because it virtualizes remote memory with the support of FPGAs. While swap-based memory disaggregation does not have a global shared address space like Kona, it has an additional address space because of the Linux kernel design. On page swaps, a local physical address has to be translated to a swap offset first in the swap address space. The corresponding remote physical address is accessed with the swap offset.

Secure address translations are not supported or undefined in most prior studies except for CXL. As CXL keeps logical device allocation metadata in *DVSEC*, which cannot be accessed by non-FM, address translation is securely protected from adversaries. However, other prior studies do not describe any mechanism to make address translation secure. The prior studies rather believe that participating nodes are trustworthy and do not violate the protocol.

Memory access pattern obfuscation: Memory disaggregation systems with direct address translations have a critical limitation that memory access patterns may leak. As the mappings between the donee’s address space and the donor’s address space are fixed, a malicious donor may track the memory access pattern of a donee by tracking the access pattern at the donor side. One of the solutions to hide memory access patterns is the Oblivious RAM (ORAM), which is an algo-

rithm that obfuscates memory access patterns from adversaries. Although there have been many studies to improve the performance of ORAM and to scale them [57, 43, 7, 11, 54], the adoption of ORAM still incurs prohibitive performance degradation in the real world. As an alternative, the existing swap system in the Linux kernel already has a sort of memory access pattern obfuscation mechanism. As the mappings between the local address space and the swap address space change on every update of pages, there is a weak relationship between the local memory access patterns and the remote memory access patterns.

2.4. FPGA

Field-programmable Gate Array (FPGA) is a device that allows the programming of on-chip hardware logic resources after fabrication. Programming of an FPGA can be done with a bitstream, which contains a sequence of commands. Modern FPGA boards support security and network features.

Security supports: As this study has been conducted with Xilinx FPGA boards, this subsection introduces the security features of Xilinx FPGAs. Xilinx FPGAs offer several security features [39]. First, bitstream encryption is a feature that encrypts a bitstream with a key. Designing an accelerator is a costly task. Therefore, there is a need to prevent unauthorized users from deploying a proprietary bitstream. When a bitstream is encrypted, the bitstream can be programmed only when a user has a valid decryption key. Second, the bitstream authentication validates a bitstream. A bitstream is authenticated with a keyed-hashed message authentication code (HMAC). Modifications to a bitstream can be detected with the HMAC. Third, disabling a JTAG port prevents tampering attempts to an FPGA. The bitstream encryption and authentication do not prevent an FPGA from being reprogrammed with an arbitrary bitstream. Reprogramming of an FPGA can be permanently blocked by disabling a JTAG port. A JTAG port can be disabled by blowing up a corresponding electronic FUSE (eFUSE).

Separate high-speed network: Modern FPGA boards are equipped with high-speed network modules. An FPGA board from Xilinx, Alveo U50, has a QSFP28 network module. The network module can be used for any network protocol as long as the protocol can be implemented in the FPGA. A network protocol can be implemented with the IP cores offered by Xilinx [9] or open-source projects [50, 47, 14]. Note that the network between FPGAs can form a physically separate network from the host’s. In other words, the network stack of FPGAs does not rely on the operating system. The direct network connection between FPGAs enables a bump-in-the-wire acceleration of incoming packets at high speed.

3. Threat Model

This study assumes a threat model where all participating nodes mutually distrust each other since our goal is to prevent the propagation of attacks across the nodes. We assume that a

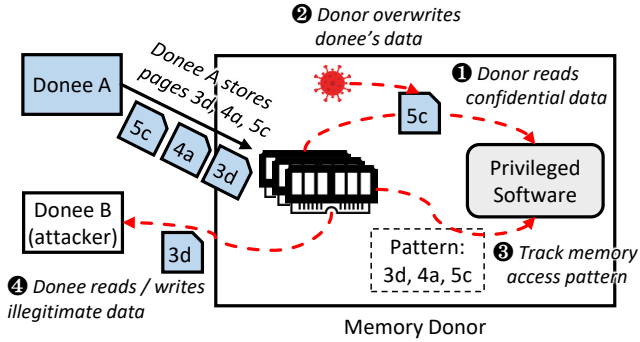


Figure 2: TDMEM threat model

donor or donee can be malicious or compromised at any time. A cloud service operator may attempt to steal the precious intellectual property of users. Alternatively, a cloud user may subvert the virtualization layer and take the root privilege. Initially, the attacker may have a limited privilege and want to gain more privileges of other nodes. Figure 2 illustrates the threat model of TDMEM. As a donor has full control of donated memory, a donor may read donees' confidential pages or overwrite them. Moreover, a compromised donor may attempt to observe which pages are written. It is not possible to identify which pages are accessed by DMA reads. However, DMA writes can be monitored indirectly by the OS. The OS can periodically read the contents of pages from the donees, and check any changes of contents. With such monitoring, the OS can identify which pages are accessed. Donees cannot be trusted either. A malicious donee may try to violate the protocol and try to read or write unauthorized pages.

All nodes are equipped with an FPGA board that implements the secure memory disaggregation engine. The bitstream is encrypted with a secret key, preventing an unauthorized node from participating in the memory disaggregation network. The authenticity of a bitstream is guaranteed by the bitstream authentication mechanism. The JTAG ports of FPGA boards are disabled after programming the bitstream. FPGA boards are assumed to be securely protected from the operating system. Once the FPGA logic is loaded, its operation is completely isolated from the operating system. The separate network path of an FPGA board allows complete isolation from the operating system. However, since the interconnects and memory are physically exposed, we do not consider physical attacks on donor or donee nodes. The availability is not guaranteed either since a malicious OS can block the operation of an FPGA board.

The trusted computing base (TCB) is defined differently by the role of a node. A donee node trusts its kernel and all FPGA boards in the system. A donee relies on the swap subsystem of the Linux kernel. Therefore, if its kernel is compromised and the kernel reads or modifies pages on the swap path, the attack cannot be eschewed. Considering that the goal of TDMEM is to prevent the propagation of attacks across nodes, the definition of the TCB is reasonable. On the

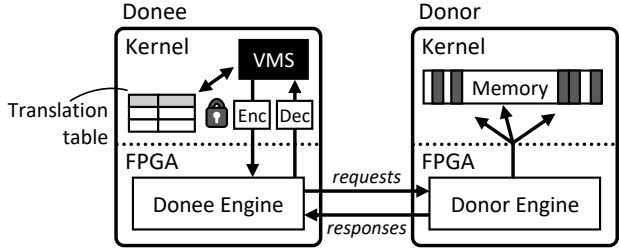


Figure 3: Overview of TDMEM

other hand, a donor node trusts all FPGA boards. It does not have to trust its or others' kernel.

4. Design

4.1. Overview

TDMEM is a disaggregated memory system with hardware supports to enhance the security of disaggregated memory. TDMEM has multiple participating nodes in a system, and each node is equipped with an FPGA board. A node can be a donor or/and donee. Workloads running in a donee can utilize the memory of remote nodes when needed.

The followings are the design goals of TDMEM.

1. The confidentiality of donees' pages is guaranteed and their integrity is validated.
2. Memory allocation is done at 4KB page granularity and memory allocation metadata is protected from malicious OSes.
3. Address translations are securely protected and cannot be bypassed or forged.
4. The memory access patterns of donees should be indistinguishable from the donor OS.

Figure 3 presents the overview of TDMEM. The donee's virtual memory system (VMS) is tightly integrated to the secure memory disaggregation engine using the frontswap interface. Frontswap allows the Linux kernel to redirect page swap requests to other subsystems. In TDMEM, the requests are redirected to the donee engine. Swap-out and swap-in commands from the donee are forwarded to its FPGA. The commands are parsed and sent to the donor engine, which is responsible for memory allocation and permission checks. On page faults, swapped-out pages are read from the donor, passing through the secure memory disaggregation engines. In the rest of this section, how the design goals are met will be described.

4.2. Confidentiality and Integrity Validation

TDMEM guarantees the confidentiality of donees' pages and validates their integrity with the donee-side software page encryption. When a page is evicted from a donee node, the page is encrypted with AES-GCM in the donee-side kernel. The encryption key is randomly generated during the initialization of TDMEM. The key resides in the kernel and is tied to

CPU		FPGA	
Encryption	Decryption	Encryption	Decryption
2.07us	2.09us	152.58us	154.62us

Table 2: AES-GCM latency comparison

a node, not shared with others. As encrypted pages cannot be read without keys, the confidentiality of pages is guaranteed. The integrity of pages can be validated by encryption also. As AES-GCM supports the authentication of encrypted data, any modifications to encrypted pages can be detected on decryption. The authentication can be done with a media authentication code (MAC). On page encryption and decryption, a MAC is generated that is unique to the page content. Therefore, once an encrypted page is modified, the MAC generated on decryption does not match to the previous one generated on encryption. MACs are stored in the donee-side address translation table.

We decide to encrypt pages in the kernel not in the FPGA because of two reasons. First, in terms of the performance and cost of memory encryption, CPUs are superior to FPGAs. Intel CPUs already have highly optimized encryption engines, which is called AES-NI [1]. AES-NI is highly optimized and operating at a very high frequency (several GHz) compared to FPGAs (200-250MHz). Table 2 compares the latencies of CPUs and FPGAs on encryption and decryption of a 4KB page. The CPU latency is measured with the `tcrypt` module in the Linux kernel. The FPGA latency is estimated with the Vitis HLS tool, where the operating frequency is set to 250MHz. We use an open-source AES-GCM implementation provided by Xilinx [53]. On CPUs, it takes 2.07us and 2.09us to encrypt and decrypt a 4KB page, respectively. On the other hand, on FPGAs, it takes 152.58us and 154.62us for encryption and decryption, respectively. Moreover, the resource utilization of encryption engines is also a problem. An AES-GCM encryption engine consumes 5.7% of LUT and 4.7% of FF. A decryption engine takes 5.9% of LUT and 5.0% of FF. Considering that the performance of the FPGA-based encryption engine is much lower than CPUs, the resource utilization is not reasonable.

4.3. Fine-grained and Secure Memory Allocation

TDMEM supports fine-grained memory allocation with the assistance of FPGAs. TDMEM has memory allocators in the secure memory disaggregation engines. In prior RDMA-based disaggregated memory, donated memory is allocated and registered at coarse-granularity in the initialization stage. Once a memory region is registered by a donee node, the allocated memory can be accessed by the node and cannot be shared with others. In such an RDMA-based system, registering memory at fine-granularity frequently is not a reasonable solution because of the excessive overheads of registering new regions [16].

An alternative way to provide secure fine-grained allocation is to use two-sided verbs of RDMA or common TCP/IP

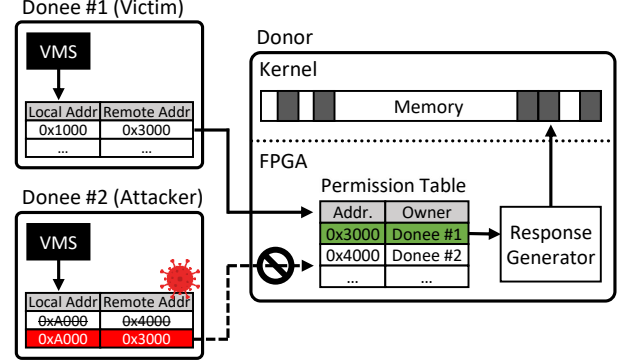


Figure 4: Decoupled translation and permission checks

network stacks. In that approach, the disaggregation software component in donor nodes will receive page access requests through networks and validate them individually. However, it can significantly increase the latency and limit the bandwidth since the software layer on the donor side must handle that. Requests and responses must be sent to the software layer by the long network stack through the NIC and operating system.

To overcome the limitation, disaggregated memory must provide an efficient page-level access control. The memory capacity of a donor node must be dynamically allocated to different donees or its own applications for efficient memory utilization. The page allocator in the donor must be nimble, and the hardware permission validation must be designed to support such page-level validation. TDMEM has memory allocators in FPGAs to allocate memory at 4KB page granularity on every page swap-out request. Memory allocators are located in FPGAs to minimize the latency on memory allocation. With FPGA-based implementation, memory allocation requests can be handled immediately once a command reaches the FPGA. The memory allocators are securely protected from malicious OSes because both the logic and metadata reside in FPGAs and cannot be altered by OSes.

4.4. Decoupled Translation and Permission Checks

Address translation must be high-performant and secure because it is in the critical path and controls memory accesses. TDMEM achieves both goals by decoupling address translations and permission checks. Figure 4 illustrates the decoupled address translation and permission checks. To achieve high-performance, TDMEM avoids introducing an additional address space. TDMEM exposes the donor's physical address space to donees directly and offloads address translations to donees. Each donee has a mapping table that maps swap offsets to remote physical addresses. By exposing the remote address space directly to donees, performance degradation is avoided. As address translations are done in donees, a compromised donor cannot forge the translation table.

The key problem with offloading address translations to donees is the risk of donees' accesses to unauthorized pages. A malicious donee may try to read illegitimate pages by tampering the translation table. TDMEM tackles the problem with

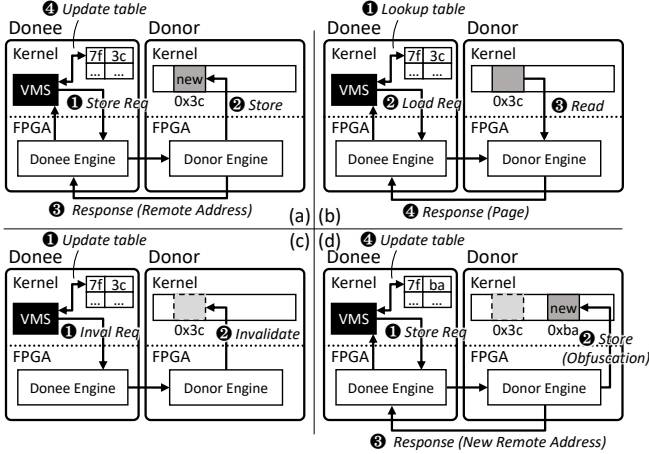


Figure 5: Memory access pattern obfuscation mechanism. Subfigure (a), (b), (c), (d) illustrate store, load, invalidate page, and store, respectively.

a permission table at the donor engine. The table tracks the ownership for all memory pages in the donor. On page loads, the permission table is looked up to validate the load request. The permission table is updated on memory allocation and deallocation. Another problem with having a permission table at the donor side is that a compromised donor may manipulate the permission table. TDMEM blocks this type of attack by having the permission table in the FPGA board. The FPGA board has a donor engine where the design is securely loaded and cannot be tampered. The integrity of the donor engine is guaranteed because the FPGA logic is protected from malicious privileged software.

4.5. Memory Access Pattern Obfuscation

TDMEM obfuscates the donees' memory access patterns to a donor. Disaggregated memory systems with direct address translations have limitations that donees' memory access patterns can be observed by a malicious donor. TDMEM overcomes this limitation with the adoption of the swap subsystem of the Linux kernel. In the Linux kernel, the swap subsystem has a swap address space in addition to the virtual and physical address spaces. The swap address space is used to allocate swap slots on swap-out requests. The swap slot (swap offset) is used to determine the location of the swapped-out page in a swap device. The allocated slot is deallocated on swap-in requests. With this swap allocation mechanism, a swap device can be fully utilized. As the mappings between the physical address between the swap address are not fixed, memory access patterns can be obfuscated.

Although the swap slot allocation logic provides a sort of obfuscation, it has a limitation that the logic is known by an attacker as the Linux kernel is open source. TDMEM overcomes the limitation by strengthening memory access pattern obfuscation with the support of FPGAs. TDMEM further obfuscates memory access patterns by changing the remote address of a local page with the secret logic implemented in FPGAs. To

integrate the logic with the Linux kernel, TDMEM borrows the commands from the frontswap interface. The frontswap interface has four commands: store, load, invalidate page, and invalidate area. On swapping out of a page, a store command is issued. On swapping in of a page, a load command and invalidate page command are generated. A load command is used to read the page from the donor. An invalidate page command deallocates the page from the donor. An invalidate area command is issued on the shutdown of a machine, which deallocates all allocated swap pages. Secret logic allocates a different page on every store command to enhance memory access pattern obfuscation.

Figure 5 illustrates how the frontswap-like interface can be used for memory access pattern obfuscation. Figure 5 (a) shows the case where a store occurs on a page, which is at 0x7f in the donee address space. The donor engine then allocates a new page at 0x3c in the remote memory, which is randomly selected among free pages. The remote address, 0x3c, is sent back to the donee engine. As shown in Figure 5 (b), on loading of the stored page, the translation table is looked up by VMS. After that, a load command is forwarded to the donor engine to load the page at 0x3c. When a page is outdated, the VMS invalidates the stored page in remote memory with invalidation, as shown in Figure 5 (c). Figure 5 (d) shows storing of the same page after invalidation. Although the donee-side page offset is the same as the previous one, a different free page on remote memory should be allocated. Such memory access pattern obfuscation prevents a malicious donor from peeking page access pattern.

5. Implementation

5.1. Overview

TDMEM is implemented in a Linux system equipped with the Xilinx Alveo U50. The FPGA board has an FPGA chip, network module, and 8GB on-board HBM. The FPGA chip is used to implement the TDMEM logic, and the network module is used to connect nodes with 100Gbps Ethernet. The role of HBM memory is determined by the role of a node. A donee uses the whole HBM memory as remote memory that can be accessed without network latency. On the other hand, a donor uses the HBM memory for donated memory and memory allocation metadata storage. The reason for this design choice will be described in the rest of this section. To summarize, TDMEM has three memory tiers: donee-HBM, donor-HBM, and donor-DRAM. On a page swap out request, a donee can specify the target memory tier to store the page. IP cores are written in Vitis HLS and Verilog, and they are integrated in the Vivado flow.

5.2. TDMEM Operations

TDMEM is tightly integrated to the virtual memory system of the Linux kernel. The integration is done with frontswap, which is the interface that redirects swap operations to other

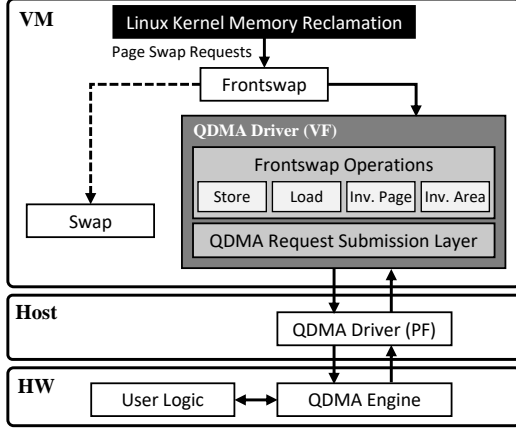


Figure 6: Software and hardware stacks of a donee

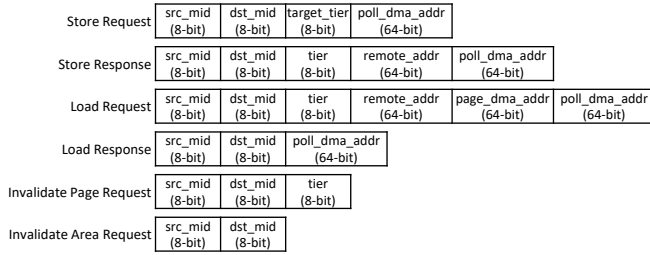


Figure 7: Command format

Command Field	Bit-width	Description
src_mid	8-bit	MID of the source machine
dst_mid	8-bit	MID of the destination machine
tier	8-bit	Memory tier where the page is stored
target_tier	8-bit	Target memory tier to store the page
remote_addr	64-bit	Memory address in the corresponding memory tier
poll_dma_addr	64-bit	DMA address of a completion
page_dma_addr	64-bit	DMA address of a page to load

Table 3: Command field descriptions

subsystems. Frontswap has four functions: store, load, invalidate page, and invalidate area. These functions become the default operations of TDMEM. On each operation, a command is generated in the kernel driver and forwarded to the donee engine over PCIe. Figure 6 illustrates the software and hardware stacks of a donee, illustrating the entire flow. Please note that the virtualization layer is used to isolate kernel driver bugs from the host machine.

The commands generated by the kernel are handled by the FPGA engines. The size of a command is 64B, which is the default transfer size of the DMA engine. A command encodes required information to process the command. The command fields and their descriptions are described in Figure 7 and Table 3. The completion of a command is identified by polling. The donee kernel is responsible for reserving a memory block that is accessible from its FPGA board. The memory block is named as `completion`, and a `completion` contains several metadata required to process the operation. A `completion` for a store command contains the completion

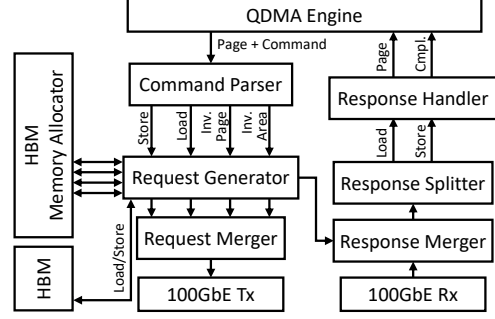


Figure 8: Block design of the donee engine

status of a request, stored memory tier, and remote memory address. These metadata are kept in the translation table in the donee. To load the page, the donee generates a request using the metadata.

5.3. Hardware Implementation

5.3.1. Common Components TDMEM uses the Xilinx QDMA Subsystem for PCI Express [42] for the communication between the host and card. QDMA is chosen over XDMA because it supports a queue-based submission mechanism, which supports thousands of concurrent requests. This feature is essential to serve concurrent page swaps. The descriptor bypass mode has been enabled to allow the card to write the host DRAM directly. For the networking feature, the UltraScale+ Integrated 100G Ethernet Subsystem [9] is used for the prototyping purpose.

5.3.2. Donee Engine The block diagram of the donee engine is illustrated in Figure 8.

Command Parser: The command parser is responsible for interpreting commands and forwarding them to the corresponding request generators. Each command has its own request generator. To forward words to the correct request generator, the command parser reads the queue ID (QID) field of the word, which is encoded by the kernel. As the command parser is aware of the QIDs of each operation, it can forward words to the correct request generator. Store commands require additional processing in the command parsing stage not to mix up requests between queues. As a store command has multiple words to convey a 4KB page, and the ordering between words is not guaranteed, words are stacked in FIFO queues so that a command can be sent as a complete packet.

Request Generator: A request generator is responsible for parsing commands and taking required actions. The store request generator stores pages in the local HBM or remote memory. The target memory tier is determined by the kernel and encoded to the command field (`target_tier`). The memory allocation status is managed by the on-board HBM memory allocator, which will be described in the following of this subsection. However, to speed up memory allocation, the store request generator pre-allocates memory and caches the addresses of several free blocks. When a store request to the local HBM fails, the request is silently redirected to the

donor engine so that memory allocation is done at the donor node. If it fails to find free memory, then the donee stores the page to a local swap device. The load request generator loads a page from the local HBM if the page is at the local HBM. Otherwise, it will forward commands to the donor engine. The invalidate page request generator and invalidate area request generator deallocate pages from the local HBM and send commands to deallocate pages from remote memory.

On-board HBM Memory Allocator: The on-board HBM memory allocator is responsible for the allocation and deallocation of on-board HBM memory. The memory allocation granularity is 4KB. The memory allocator is implemented with a bitmap. As the size of HBM is 8GB, the size of the bitmap is 2,097,152-bit (256KB). To allow concurrent access to the table, `ARRAY_PARTITION` pragma has been applied to the table with a cyclic option and factor of 32.

Response Handler: The response handler reads returned responses and writes completions or pages to the donee. Only two commands have responses: store and load. The completion of page invalidation does not have to be identified. The identification of page invalidation results in wasted hardware resource and network bandwidth. A store response is a single-word response that contains the tier and address of the stored page. A load packet has 65 words, where the first word has the metadata, and the following 64 words have the page content. The writes from the store response handler and load response handler are arbitrated in a round-robin manner.

5.3.3. Donor Engine Unlike the donee engine, where commands are sent from the host side, the donor engine receives commands from the network interface. Figure 9 presents the block design of the donor engine.

Request Splitter & Response Generator: After receiving requests from the network module, the requests are split by the request splitter. The request splitter reads the command field and forwards requests to the corresponding response generators. The response generators are different from the donee-side request generators in two aspects. First, the response generators coordinate not only with the on-board HBM memory allocator but also with the host DRAM memory allocator. Second, the invalidate page response generator and invalidate area response generator do not generate response packets. The store response generator and load response generator access donated memory, which is reserved by the kernel. The donor reserves memory with the kernel boot parameter, `memmap`. The donor engine knows the starting address and the size of the donated memory.

On-board HBM Allocator & Host DRAM Allocator: The donor-side memory allocators have the same responsibility as the donee-side's, which is to manage the allocation status of memory. However, there are two differences from the donee-side memory allocator. First, the donor-side memory allocator has to track the ownership of pages in addition to allocation status. The load response generator looks up the memory allocator to confirm that the current load request is trying

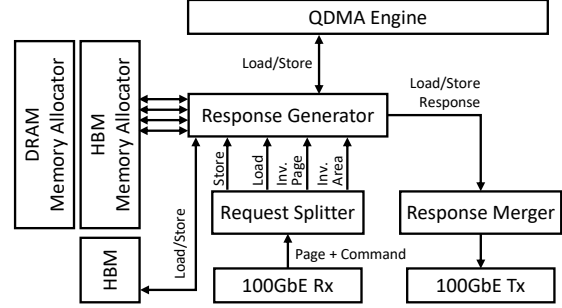


Figure 9: Block design of the donor engine

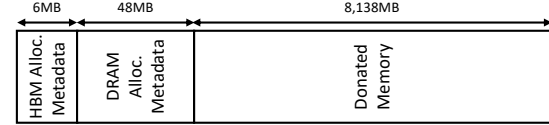


Figure 10: Donor-side HBM memory map

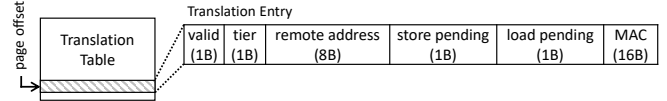


Figure 11: Translation table entry format

to read a valid memory page that is owned by the requestor. The ownership of pages is tracked with a machine ID (MID), whose size is 8-bit. As the metadata size becomes eight times of the donee side's, it is not possible to hold all metadata in the FPGA logic. Instead, the metadata is stored in the lower address of the HBM. Figure 10 presents the HBM memory map. Second, the donor engine has the host DRAM memory allocator in addition to the on-board HBM memory allocator.

5.4. Software Implementation

5.4.1. Address Translation TDMEM offloads the address translation responsibility to donees. Each donee has a flat address translation table that maps a local address (swap offset) to a remote physical. Figure 11 presents the format of the translation entry. The `valid` field presents whether the entry has valid translation information. A translation entry becomes valid when a store request completes. The `tier` field presents the memory tier where the page is stored, and the `remote_address` field has the address of the page in the tier. The `store_pending` and `load_pending` fields are used to coordinate with other concurrent swap requests. The fields are used to prevent loading pages before store completion or invalidating pages before page load completion. The `MAC` field is used for the authentication of decrypted pages. The field is updated on encryption. The `MAC` field is compared with the MAC that is generated on the decryption of the page.

5.4.2. Software Page Encryption Pages are encrypted in the donee's kernel with AES-GCM on stores. The encryption key and initialization vectors are generated in the initialization stage of the donee. The AES-GCM algorithm takes associated data as an input for validation. The swap offset of the page is used for the associated data. Pages are decrypted on page

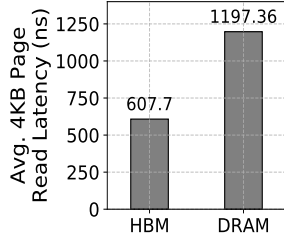


Figure 12: On-FPGA 4KB page read latency, which excludes the overhead of the software and network stack

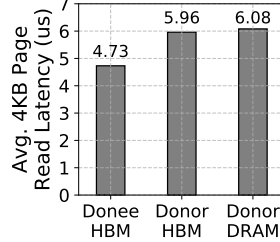


Figure 13: Donee-side 4KB page read latency, which includes the overhead of the software and network stack

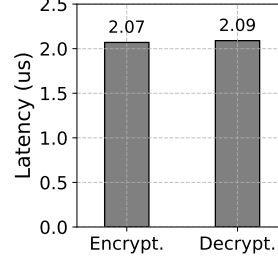


Figure 14: 4KB page encryption latency and decryption latency

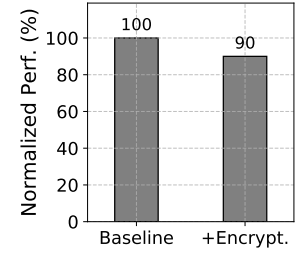


Figure 15: The impact of memory encryption on the microbenchmark performance

	Donor Host	Donee Host	Donee Guest
Memory	DDR4 188GB	DDR4 125GB	DDR4 32GB
Kernel		5.9.0	5.10.0
Processors	Intel(R) Xeon(R) CPU E5-2630 v4		
OS		Ubuntu 18.04	
QDMA Driver		2020.2	

Table 4: System configurations

Workload Name	Mem. Footprint (GB)	Num of CPUs
tensorflow-inception	1.5	2
kmeans	5.3	8
quicksort	8.6	1
in-memory-analytics	7.6	8
graph-analytics	10.3	8
xsbench	5.5	8

Table 5: Macrobenchmarks and their memory footprint

loads, and the MAC is compared to the one generated during the encryption. MAC is stored in the translation entry of the page, and if the MAC mismatches, TDMEM stops serving the page fault, and the system halts.

6. Evaluation

6.1. Experimental Setup

We evaluate the performance of TDMEM on a Linux system equipped with an FPGA card and high-performance network card. The evaluation is conducted with two pairs of machines. The first pair of machines is equipped with Mellanox ConnectX-5 for the evaluation of fastswap. The second pair of machines has Xilinx Alveo U50 to evaluate TDMEM. In each pair, one machine becomes a donor and the other becomes a donee. Table 4 presents the machines and their configurations. Table 5 presents the evaluated macrobenchmarks. The table shows their memory footprint and the number of CPUs that they utilize.

6.2. Microbenchmark Results

6.2.1. On-FPGA Page Read Latency Figure 12 presents the 4KB page read latency where the software overhead is not included. The page read latency is measured by designing and deploying a microbenchmark in the FPGA. The microbench-

mark module reads 4KB pages sequentially for a given range of memory addresses. The total elapsed cycles are measured, and the elapsed cycles are divided by the number of pages read. As the microbenchmark is designed to operate at 250MHz, the clock period is 4ns. The average 4KB page read latency is calculated by multiplying the clock period by the average elapsed cycles. On average, HBM takes 607.7ns, and DRAM takes 1197.36ns to read a 4KB page.

6.2.2. Donee-side Page Read Latency Unlike the previous experiment, which excludes the overhead of the software and network stacks, this experiment includes them by measuring the page read latency in the donee-side Linux kernel. Figure 13 presents the average page read latency in three types of memory tiers: donee-HBM, donor-HBM, and donor-DRAM. The page read latency has been measured by sequentially reading 2,097,152 pages (8GB) from the target memory tier. The pages are stored in the target memory before running experiments, and the elapsed time has been measured with jiffies in the Linux kernel. `CONFIG_HZ`, which is the kernel configuration that defines the timer resolution, is set to 250. The experiment result implies that the performance gap between HBM and DRAM presented in Figure 12 is mostly hidden, and the performance overhead comes from the network latency and page fault handling.

6.2.3. Page Encryption Latency We measured the page encryption latency in the Linux kernel. The vanilla Linux kernel has the `tcrypt` module, which evaluates the performance of encryption algorithms. We evaluated the performance of `gcm(aes)` with the key size of 128-bit. Figure 14 presents the average page encryption and decryption latencies. It takes 2.07us for 4KB page encryption and 2.09us for 4KB page decryption. Although the latency seems relatively high considering that the latency of page read is between 4-6us, most of the latency can be hidden by the readahead mechanism of the Linux kernel.

Figure 15 shows the normalized performance of a microbenchmark that loads 262,144 pages (1GB) sequentially from the donee HBM. The normalized performance is defined as the performance normalized to the baseline without encryption. The performance is the reverse of the elapsed

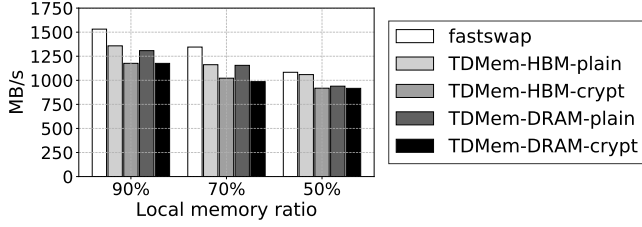


Figure 16: Memory bandwidth measured with the STREAM Triad benchmark

time. The performance of the microbenchmark with page encryption shows 90% of the performance without encryption. Most pages are readahead and decrypted in the swap cache, effectively hiding the memory decryption latency.

6.2.4. Memory Bandwidth In this experiment, we measure the memory bandwidth of TDMEM and compare it with fastswap’s. The memory bandwidth is measured with the STREAM benchmark. STREAM allocates 4GB memory and runs several sub-benchmarks to measure the bandwidth. Among the sub-benchmarks, we use the Triad to measure the average memory bandwidth. We measure the memory bandwidth of five configurations: fastswap, TDMem-HBM-plain, TDMem-HBM-crypt, TDMem-DRAM-plain, and TDMem-DRAM-crypt. fastswap presents the case where the swapped-out pages are stored in remote memory with RDMA. The configurations starting with TDMem is run with TDMEM. The HBM and DRAM keywords show the target memory tier where the swapped-out pages are stored at. The crypt keyword means that the encryption latency is added on page loads. The experiments are run with various local memory ratios, which include 90%, 70%, and 50%. The local memory ratio is defined as the memory size in the donee DRAM divided by the maximum memory footprint size. The memory footprint has been measured with the cgroup’s `memory.usage_in_bytes`.

Figure 16 shows the memory bandwidth with the configurations. fastswap performs the best with the 90% and 70% local memory ratios. At the 90% local memory ratio, fastswap, TDMem-HBM-crypt, and TDMem-DRAM-crypt present 1531.6MB/s, 1261.4MB/s, 1210.4MB/s, respectively. Please note that the memory bandwidth gap between TDMem-HBM-crypt and TDMem-DRAM-crypt is negligible, implying that the major bottleneck for the memory bandwidth is not the memory itself. The memory bandwidth loss of TDMem-DRAM-crypt compared to fastswap are 21%, 19%, and 3% at the 90%, 70%, and 50% local memory ratio, respectively.

6.3. Macrobenchmark Results

Geomean of normalized performance: Figure 17 presents the geomean of normalized performance of workloads for a given configuration. The normalized performance is defined as the performance of a workload with a given configuration divided by the performance of the workload run with 100%

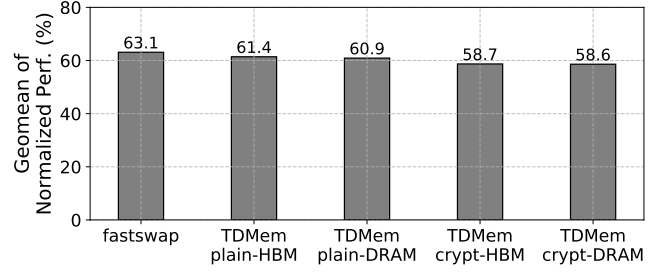


Figure 17: Geomean of normalized performance of workloads for each configuration

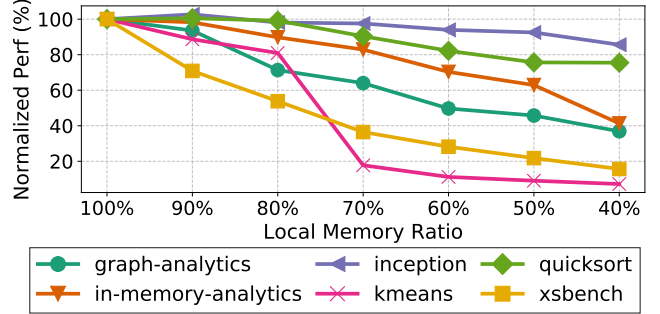


Figure 18: Normalized performance of workloads with various local memory ratios with TDMEM. Swapped out pages are stored in the donor DRAM

local memory. The geomean of normalized performance is the geomean of all normalized performance of workloads. Workloads are run with five configurations: fastswap, TDMem-HBM-plain, TDMem-HBM-crypt, TDMem-DRAM-plain, and TDMem-DRAM-crypt. The experiments are run while varying the local memory ratio between 40% and 100% with the 10% step size. Fastswap shows 64.5% performance compared to the non-swapped run, and TDMEM experiences negligible performance loss, presenting the 3-5% lower performance compared to fastswap. Please note that the performance overhead from software encryption is mostly hidden because of the readahead mechanism in the Linux kernel, as we have shown in Section 6.2.3.

Normalized performance (TDMem-DRAM-crypt): Among the experiment configurations presented in Figure 17, we choose TDMem-DRAM-crypt and illustrate workloads’ performance degradation while varying the local memory ratio in Figure 18. The performance loss from losing local memory differs for each workload. While in-memory-analytics presents 70% of its performance with the 40% local memory ratio, kmeans shows 6.3% of its performance. We qualitatively analyze the root cause with the tools presented in prior studies [38, 19], which allow us to analyze the memory access frequency. We found that the reason behind the different sensitivity on the local memory ratio is the various memory access patterns and intensity. While the memory footprint of in-memory-analytics is

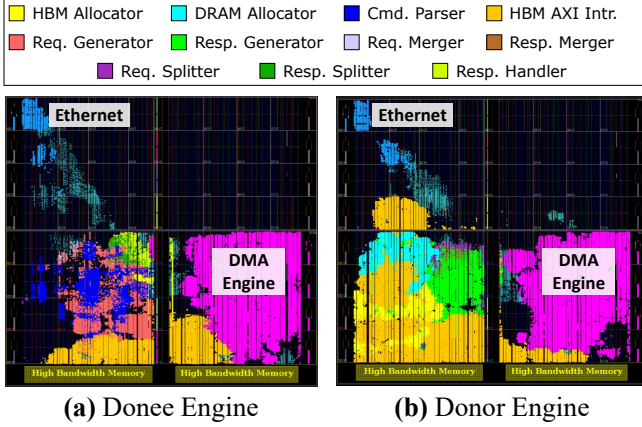


Figure 19: Floorplan of TDMEM

Donee Resource Utilization Breakdown (%)					
Component	LUT	LUTMEM	FF	BRAM	URAM
DMA Engine	47.8	48.0	40.3	23.6	100.0
Cmd Parser	6.7	0.0	11.8	35.5	0.0
Req Generator	13.4	1.5	11.4	19.8	0.0
HBM Alloc	0.4	0.0	0.3	15.8	0.0
HBM AXI Intr.	10.3	37.7	19.5	0.0	0.0
Req Merger	0.3	0.0	0.0	0.0	0.0
Ethernet	0.8	1.5	1.4	0.0	0.0
Rsp Merger	0.2	0.0	0.0	0.0	0.0
Rsp Splitter	0.6	0.0	1.7	0.0	0.0
Rsp Handler	0.6	0.0	1.7	0.0	0.0
Others	18.8	11.3	11.9	5.3	0.0

Donor Resource Utilization Breakdown (%)					
Component	LUT	LUTMEM	FF	BRAM	URAM
DMA Engine	43.2	27.9	28.0	29.4	100.0
Req Splitter	0.7	0.0	1.2	0.0	0.0
Rsp Generator	10.1	1.7	9.9	51.4	0.0
DRAM Alloc	6.4	2.4	7.7	3.6	0.0
HBM Alloc	6.4	2.4	7.7	3.6	0.0
HBM AXI Intr.	27.5	57.5	35.4	0.0	0.0
Rsp Merger	0.2	0.0	0.0	0.0	0.0
Ethernet	0.7	0.9	1.0	0.0	0.0
Others	4.7	7.1	9.1	11.9	0.0

Table 6: Resource utilization breakdown of TDMEM

10.6GB, only 2GBs of memory is intensively accessed. On the other hand, the total allocated memory of k_{means} is intensively accessed, being more sensitive to the local memory loss.

6.4. FPGA Resource Utilization

Figure 19 illustrates the floorplan of the donee engine and donor engine, and each component is filled with different colors. The donee engine consumes 18% of LUT, 5% of LUTRAM, 12% of FF, 30% of BRAM, and 2% of URAM. The donor engine accounts for 19% of LUT, 9% of LUTRAM, 17% of FF, 24% of BRAM, and 2% of URAM. As it can be seen in the figure, there is enough room for additional hardware components. Table 6 presents the breakdown of logic resource consumption for each engine. Each row presents the

ratio of consumed logic resources out of the total resource consumption of the engine. In both engines, DMA engines are the major consumer of logic resources. In the donee engine, the HBM memory allocator accounts for 15.8% of the BRAM consumption of the donee engine. BRAM is used to manage the memory allocation status of HBM memory. On the other hand, as the donor engine manages the memory allocation status in the on-board HBM, the BRAM usage of memory allocators is relatively low. The response generator consumes BRAM for the free lists in the store response generator. All BRAMs in the response generator are consumed by the store response generator.

7. Related Work

FPGA is drawing the attention of the computer architecture community and system community. From the architecture perspective, FPGA is an attractive option to model custom accelerators before diving into the ASIC design. Prototyping the performance of accelerators with FPGAs has been done in neural network accelerators [48, 31, 21, 8] and sparse matrix multiplication accelerators [12, 29, 17, 20]. From the system perspective, it opens a new design space such as virtualization and resource management [58, 25, 49, 27]. Designing a system with FPGAs is more than a pure academic study. Microsoft Catapult project [41, 5, 15, 13] has shown that FPGAs can improve the performance of real-world applications.

In swap-based disaggregated memory systems, the page replacement algorithm plays an important role in identifying cold pages and swapping out them to remote memory. Although there have been many theoretical studies to improve the page replacement policies [44, 35, 52, 28, 32, 3, 23, 24], the Linux kernel page replacement algorithm sticks to the LRU lists that mostly rely on heuristics in practice. Moreover, the page replacement algorithm has been designed in the context of swapping pages to a slow disk, which is quite different from the emerging memory systems. A few recent studies tried to optimize the page replacement policy in the context of tiered memory systems [56, 19], and Google shared the improvement for page replacement, the multi-generational LRU [33, 34] to the Linux kernel community.

8. Conclusion

This paper proposes a new hardware-assisted memory disaggregation system, TDMEM. It allows fine-grained page-level management of memory pools in donor nodes, while access validation is enforced by the secure hardware engine protected from vulnerable operating systems. In addition, it further secures the confidentiality of memory pages with page address oblivious supports as well as encryption. The security features of TDMEM cause a negligible performance overhead, which causes 4.4% performance degradation compared to the latest page-granular far memory system, fastswap. Although our prototype is built upon an FPGA-based system, it can be de-

signed for ASICs with higher performance. Our evaluation with FPGA implementation showed that such fine-grained secure disaggregated memory is feasible with comparable performance to the latest software-based techniques.

9. Acknowledgment

This work was supported by the National Research Foundation of Korea (NRF-2019R1A2B5B01069816) and the Institute for Information & Communications Technology Promotion (IITP2017-0-00466). Both grants are funded by the Ministry of Science and ICT, Korea.

References

- [1] Kahraman Akdemir, Martin Dixon, Wajdi Feghali, Patrick Fay, Vinodh Gopal, Jim Guilford, Erdinc Ozturk, Gil Wolrich, and Ronen Zohar. Breakthrough AES performance with intel AES new instructions. *White paper*, June, 2010.
- [2] Emmanuel Amaro, Christopher Branner-Augmon, Zhihong Luo, Amy Ousterhout, Marcos K Aguilera, Aurojit Panda, Sylvia Ratnasamy, and Scott Shenker. Can Far Memory Improve Job Throughput? In *Proceedings of the 15th European Conference on Computer Systems (EuroSys)*, 2020.
- [3] Sorav Bansal and Dharmendra S Modha. CAR: Clock with Adaptive Replacement. In *Proceedings of the 3rd USENIX Conference on File and Storage Technologies (FAST)*, pages 187–200, 2004.
- [4] Irina Calciu, Talha Imran, Ivan Puddu, Sanidhya Kashyap, Hasan Maruf, Onur Mutlu, and Aasheesh Kolli. Rethinking Software Runtimes for Disaggregated Memory. In *Proceedings of the 26th International Conference on Architectural Support for Programming Languages and Operating Systems (ASPLOS)*, 2021.
- [5] Adrian M Caulfield, Eric S Chung, Andrew Putnam, Hari Angepat, Jeremy Fowers, Michael Haselman, Stephen Heil, Matt Humphrey, Puneet Kaur, Joo-Young Kim, et al. A Cloud-Scale Acceleration Architecture. In *Proceedings of the 49th International Symposium on Microarchitecture (MICRO)*, 2016.
- [6] CCIX Consortium. <https://www.ccixconsortium.com/>. [Online; accessed 4-August-2019].
- [7] T-H Hubert Chan and Elaine Shi. Circuit OPRAM: Unifying statistically and computationally secure ORAMs and OPRAMs. In *Proceedings of the Conference on Theory of Cryptography*, 2017.
- [8] Sung-En Chang, Yanyu Li, Mengshu Sun, Runbin Shi, Hayden K-H So, Xuehai Qian, Yanzhi Wang, and Xue Lin. Mix and Match: A Novel FPGA-Centric Deep Neural Network Quantization Framework. In *Proceedings of the 27th International Symposium on High Performance Computer Architecture (HPCA)*, 2021.
- [9] UltraScale+ Integrated 100G Ethernet Subsystem. https://www.xilinx.com/products/intellectual-property/cmac_usplus.html. [Online; accessed 6-April-2021].
- [10] Compute Express Link (CXL). <https://www.computeexpresslink.org/>. [Online; accessed 4-August-2019].
- [11] Jack Doerner and Abhi Shelat. Scaling ORAM for Secure Computation. In *Proceedings of the Conference on Computer and Communications Security (CCS)*, 2017.
- [12] Yousef Elkurdi, David Fernández, Evgueni Souleimanov, Dennis Giannacopoulos, and Warren J Gross. FPGA architecture and implementation of sparse matrix-vector multiplication for the finite element method. *Computer Physics Communications*, 178(8), 2008.
- [13] Daniel Firestone, Andrew Putnam, Sambhrama Mundkur, Derek Chiou, Alireza Dabagh, Mike Andrewartha, Hari Angepat, Vivek Bhanu, Adrian Caulfield, Eric Chung, et al. Azure Accelerated Networking: SmartNICs in the Public Cloud. In *Proceedings of the 15th USENIX Symposium on Networked Systems Design and Implementation (NSDI)*, 2018.
- [14] Alex Forencich, Alex C Snoeren, George Porter, and George Papen. Corundum: An Open-Source 100-Gbps NIC. In *Proceedings of the 28th Annual International Symposium on Field-Programmable Custom Computing Machines (FCCM)*, 2020.
- [15] Jeremy Fowers, Kalin Ovtcharov, Michael Papamichael, Todd Masegill, Ming Liu, Daniel Lo, Shlomi Alkalay, Michael Haselman, Logan Adams, Mahdi Ghandi, et al. A Configurable Cloud-Scale DNN Processor for Real-Time AI. In *Proceedings of the 45th International Symposium on Computer Architecture (ISCA)*, 2018.
- [16] Philip Werner Frey and Gustavo Alonso. Minimizing the Hidden Cost of RDMA. In *2009 29th IEEE International Conference on Distributed Computing Systems*, 2009.
- [17] Paul Grigoraş, Pavel Burovskiy, Wayne Luk, and Spencer Sherwin. Optimising Sparse Matrix Vector multiplication for large scale FEM problems on FPGA. In *Proceedings of the International Conference on Field Programmable Logic and Applications (FPL)*, 2016.
- [18] Juncheng Gu, Youngmoon Lee, Yiwen Zhang, Mosharaf Chowdhury, and Kang G Shin. Efficient Memory Disaggregation with Infiniswap. In *Proceedings of the 14th USENIX Symposium on Networked Systems Design and Implementation (NSDI)*, 2017.
- [19] T. Heo, Y. Wang, W. Cui, J. Huh, and L. Zhang. Adaptive page migration policy with huge pages in tiered memory systems. *IEEE Transactions on Computers*, pages 1–1, 2020.
- [20] Reza Hojabr, Ali Sedaghati, Amirali Sharifian, Ahmad Khonsari, and Arrvinth Shriraman. SPAGHETTI: Streaming Accelerators for Highly Sparse GEMM on FPGAs. In *Proceedings of the 27th International Symposium on High Performance Computer Architecture (HPCA)*, 2021.
- [21] Ranggi Hwang, Taehun Kim, Youngeun Kwon, and Minsoo Rhu. Centaur: A Chiplet-based, Hybrid Sparse-Dense Accelerator for Personalized Recommendations. In *Proceedings of the 47th International Symposium on Computer Architecture (ISCA)*, 2020.
- [22] Mohammad Saiful Islam, Mehmet Kuzu, and Murat Kantarcioglu. Access Pattern disclosure on Searchable Encryption: Ramification, Attack and Mitigation. In *Proceedings of the Symposium on Network and Distributed System and Security (NDSS)*, 2012.
- [23] Song Jiang, Feng Chen, and Xiaodong Zhang. CLOCK-Pro: An Effective Improvement of the CLOCK Replacement. In *USENIX Annual Technical Conference (ATC)*, pages 323–336, 2005.
- [24] Song Jiang and Xiaodong Zhang. LIRS: An Efficient Low Inter-reference Recency Set Replacement Policy to Improve Buffer Cache Performance. In *Proceedings of the 2002 ACM SIGMETRICS International Conference on Measurement and Modeling of Computer Systems*, pages 31–42, 2002.
- [25] Ahmed Khawaja, Joshua Landgraf, Rohith Prakash, Michael Wei, Eric Schkufza, and Christopher J Rossbach. Sharing, Protection, and Compatibility for Reconfigurable Fabric with AmorphOS. In *Proceedings of the 13th Symposium on Operating Systems Design and Implementation (OSDI)*, 2018.
- [26] Vamsee Reddy Kommareddy, Clayton Hughes, Simon David Hammond, and Amro Awad. DeACT: Architecture-Aware Virtual Memory Support for Fabric Attached Memory Systems. In *Proceedings of the 27th International Symposium on High Performance Computer Architecture (HPCA)*, 2021.
- [27] Dario Korolija, Timothy Roscoe, and Gustavo Alonso. Do OS abstractions make sense on FPGAs? In *Proceedings of the 14th Symposium on Operating Systems Design and Implementation (OSDI)*, 2020.
- [28] Donghee Lee, Jongmoo Choi, Jong-Hun Kim, Sam H Noh, Sang Lyul Min, Yookun Cho, and Chong Sang Kim. LRFU: A Spectrum of Policies that Subsumes the Least Recently Used and Least Frequently Used Policies. *IEEE Transactions on Computers*, 50(12):1352–1361, 2001.
- [29] Colin Yu Lin, Ngai Wong, and Hayden Kwok-Hay So. Design space exploration for sparse matrix-matrix multiplication on FPGAs. *International Journal of Circuit Theory and Applications*, 41(2), 2013.
- [30] Martin Maas, Eric Love, Emil Stefanov, Mohit Tiwari, Elaine Shi, Krste Asanovic, John Kubiatowicz, and Dawn Song. PHANTOM: Practical Oblivious Computation in a Secure Processor. In *Proceedings of the Conference on Computer and Communications Security (CCS)*, pages 311–324, 2013.
- [31] Divya Mahajan, Jongse Park, Emmanuel Amaro, Hardik Sharma, Amir Yazdanbakhsh, Joon Kyung Kim, and Hadi Esmaeilzadeh. TABLA: A Unified Template-based Framework for Accelerating Statistical Machine Learning. In *Proceedings of the 22nd International Symposium on High Performance Computer Architecture (HPCA)*, 2016.
- [32] Nimrod Megiddo and Dharmendra S Modha. ARC: A Self-Tuning, Low Overhead Replacement Cache. In *Proceedings of the 2nd USENIX Conference on File and Storage Technologies (FAST)*, pages 115–130, 2003.
- [33] The multi-generational LRU. <https://lwn.net/Articles/851184/>. [Online; accessed 15-April-2021].
- [34] [PATCH v1 00/14] Multigenerational LRU. <https://lwn.net/ml/linux-kernel/20210313075747.3781593-1-yuzhao@google.com/>. [Online; accessed 15-April-2021].

- [35] Elizabeth J O’neil, Patrick E O’neil, and Gerhard Weikum. The LRU-K Page Replacement Algorithm for Database Disk Buffering. In *Proceedings of the 1993 ACM SIGMOD International Conference on Management of Data*, pages 297–306, 1993.
- [36] OpenCAPI. <https://opencapi.org/>. [Online; accessed 4-August-2019].
- [37] Dag Arne Osvic, Adi Shamir, and Eran Tromer. Cache Attacks and Countermeasures: The Case of AES. In *Topics in Cryptology – CT-RSA 2006*, 2006.
- [38] SeongJae Park, Yunjae Lee, and Heon Y Yeom. Profiling Dynamic Data Access Patterns with Controlled Overhead and Quality. In *Proceedings of the 20th International Middleware Conference Industrial Track*, 2019.
- [39] Ed Peterson. Developing Tamper Resistant Designs with Xilinx Virtex-6 and 7 Series FPGAs. *Application Note. Xilinx Corporation*, 2013.
- [40] Christian Pinto, Dimitris Syrivelis, Michele Gazzetti, Panos Koutsosavasilis, Andrea Reale, Kostas Katrinis, and H Peter Hofstee. Thymesis-Flow: A Software-Defined, HW/SW co-Designed Interconnect Stack for Rack-Scale Memory Disaggregation. In *Proceedings of the 53rd International Symposium on Microarchitecture (MICRO)*, 2020.
- [41] Andrew Putnam, Adrian M Caulfield, Eric S Chung, Derek Chiou, Kypros Constantinides, John Demme, Hadi Esmaeilzadeh, Jeremy Fowers, Gopi Prashanth Gopal, Jan Gray, et al. A Reconfigurable Fabric for Accelerating Large-Scale Datacenter Services. In *Proceedings of the 41st International Symposium on Computer Architecture (ISCA)*, 2014.
- [42] QDMA Subsystem for PCI Express. <https://www.xilinx.com/products/intellectual-property/pcie-qdma.html>. [Online; accessed 6-April-2021].
- [43] Ling Ren, Christopher Fletcher, Albert Kwon, Emil Stefanov, Elaine Shi, Marten Van Dijk, and Srinivas Devadas. Constants Count: Practical Improvements to Oblivious RAM. In *Proceedings of the 24th USENIX Security Symposium*, 2015.
- [44] John T Robinson and Murthy V Devarakonda. Data Cache Management using Frequency-based Replacement. In *Proceedings of the 1990 ACM SIGMETRICS International Conference on Measurement and Modeling of Computer Systems*, pages 134–142, 1990.
- [45] Benjamin Rothenberger, Konstantin Taranov, Adrian Perrig, and Torsten Hoefler. RedMark: Bypassing RDMA Security Mechanisms. In *Proceedings of the 30th USENIX Security Symposium (Security)*, 2021.
- [46] Zhenyuan Ruan, Malte Schwarzkopf, Marcos K Aguilera, and Adam Belay. AIFM: High-Performance, Application-Integrated Far Memory. In *Proceedings of the 14th Symposium on Operating Systems Design and Implementation (OSDI)*, 2020.
- [47] Mario Ruiz, David Sidler, Gustavo Sutter, Gustavo Alonso, and Sergio López-Buedo. Limago: An FPGA-Based Open-Source 100 GbE TCP/IP Stack. In *Proceedings of the 29th International Conference on Field Programmable Logic and Applications (FPL)*, 2019.
- [48] Hardik Sharma, Jongse Park, Divya Mahajan, Emmanuel Amaro, Joon Kyung Kim, Chenkai Shao, Asit Mishra, and Hadi Esmaeilzadeh. From High-Level Deep Neural Models to FPGAs. In *Proceedings of the 49th International Symposium on Microarchitecture (MICRO)*, 2016.
- [49] Ran Shu, Peng Cheng, Guo Chen, Zhiyuan Guo, Lei Qu, Yongqiang Xiong, Derek Chiou, and Thomas Moscibroda. Direct Universal Access: Making Data Center Resources Available to FPGA. In *Proceedings of the 16th USENIX Symposium on Networked Systems Design and Implementation (NSDI)*, 2019.
- [50] David Sidler, Gustavo Alonso, Michaela Blott, Kimon Karras, Kees Vissers, and Raymond Carley. Scalable 10Gbps TCP/IP Stack Architecture for Reconfigurable Hardware. In *Proceedings of the 23rd International Symposium on Field-Programmable Custom Computing Machines*, 2015.
- [51] Anna Kornfeld Simpson, Adriana Szekeres, Jacob Nelson, and Irene Zhang. Securing RDMA for High-Performance Datacenter Storage Systems. In *Proceedings of the 12th USENIX Workshop on Hot Topics in Cloud Computing (HotCloud)*, 2020.
- [52] Yannis Smaragdakis, Scott Kaplan, and Paul Wilson. EELRU: Simple and Effective Adaptive Page Replacement. In *Proceedings of the 1999 ACM SIGMETRICS International Conference on Measurement and Modeling of Computer Systems*, pages 122–133, 1999.
- [53] Vitis Accelerated Libraries. https://github.com/Xilinx/Vitis_Libraries. [Online; accessed 20-July-2019].
- [54] Rujia Wang, Youtao Zhang, and Jun Yang. Cooperative Path-ORAM for Effective Memory Bandwidth Sharing in Server Settings. In *Proceedings of the 23rd International Symposium on High Performance Computer Architecture (HPCA)*, 2017.
- [55] Yuanzhong Xu, Weidong Cui, and Marcus Peinado. Controlled-Channel Attacks: Deterministic Side Channels for Untrusted Operating Systems. In *Proceedings of the Symposium on Security and Privacy*, 2015.
- [56] Zi Yan, Daniel Lustig, David Nellans, and Abhishek Bhattacharjee. Nimble Page Management for Tiered Memory Systems. In *Proceedings of the 24th International Conference on Architectural Support for Programming Languages and Operating Systems (ASPLOS)*, 2019.
- [57] Xiangyao Yu, Syed Kamran Haider, Ling Ren, Christopher Fletcher, Albert Kwon, Marten Van Dijk, and Srinivas Devadas. PrORAM: Dynamic Prefetcher for Oblivious RAM. In *Proceedings of the 42nd Annual International Symposium on Computer Architecture (ISCA)*, 2015.
- [58] Jiansong Zhang, Yongqiang Xiong, Ningyi Xu, Ran Shu, Bojie Li, Peng Cheng, Guo Chen, and Thomas Moscibroda. The Feniks FPGA Operating System for Cloud Computing. In *Proceedings of the 8th Asia-Pacific Workshop on Systems*, 2017.
- [59] Xiaotong Zhuang, Tao Zhang, and Santosh Pande. HIDE: An Infrastructure for Efficiently Protecting Information Leakage on the Address Bus. In *Proceedings of the 9th International Conference on Architectural Support for Programming Languages and Operating Systems (ASPLOS)*, 2004.